Decreased peak tailing during transport of solutes in porous media with alternate adsorption properties

Rana, C.; De Malsche, W.; De Wit, A.

Published in:
Chemical Engineering Science

DOI:
10.1016/j.ces.2019.04.003

Publication date:
2019

Decreased peak tailing during transport of solutes in porous media with alternate adsorption properties

C. Rana[1], W. De Malsche[2] and A. De Wit[1]

[1] *Nonlinear Physical Chemistry Unit, Université libre de Bruxelles (ULB), 1050 Brussels, Belgium.* [2]*Department of Chemical Engineering, Vrije Universiteit Brussel (VUB), Pleinlaan 2, 1050 Brussels, Belgium*

Abstract

In adsorption based separation techniques or in environmental applications where adsorption on a porous matrix is involved, the broadening of migrating bands of solutes varies with the characteristics of the adsorption isotherms~~. For nonlinear Langmuir (L) adsorption isotherms, the displacement speed of the solutes decreases when their concentration in the mobile phase increases, inducing a sharpening of the frontal part of the spatial concentration peak and a tailing at its back. A reverse effect, i.e. formation of a shock layer at the back and widening at the frontal part of the spatial concentration peak, is obtained for nonlinear anti-Langmuir (AL) isotherms typically observed in overloading conditions at high analyte concentrations. We~~ and is generally overwhelming at solute concentrations deep in the non-linear region. We introduce here a novel concept to minimize concentration overloading dispersion: We show theoretically that a spatial alternation of Langmuir (L) and Anti-Langmuir (AL) zones along the displacement direction induces an accordion effect, i.e. an alternation of sharpening and dilution of the solute zones, reducing in the end the final broadening of the peak. ~~To do so, we~~

~~develop a model describing the displacement of a given solute in a porous matrix alternating L and AL adsorption zones and~~ We quantify in the parameter space of the problem the reduction in ~~band broadening~~ concentration overloading related band widening of the L-AL system compared to the pure L or AL cases. A numerical analysis of the solute transport reveals a dependence of solute spreading on the ratio of sample to ~~plate~~ stationary phase zone widths and on the intensity of the adsorption parameter. The initial position of the sample solvent in its surrounding liquid i.e. whether the displacement starts in a L or AL zone is also shown to have an influence on the dispersive behavior. An ~~optimization~~ analysis is performed to highlight the optimal alternance geometry to minimize solute spreading.
Keywords: Heterogeneous porous media, Langmuir adsorption, anti-Langmuir adsorption, accordion effect, chromatography, spreading, peak tailing

1. Introduction

In porous media, understanding the transport of solutes that can adsorb on the porous matrix is of importance for environmental applications as, for instance, in carbon capture and sequestration [1], oil recovery [2] or contaminant remediation in subsurface systems [3, 4]. In chemical and pharmaceutical engineering, processes such as chromatographic separation of solutes from a mixture also exploit transport and adsorption in porous systems to obtain high purity compounds [5, 6]. ~~Such adsorption or interaction based separation methods are versatile and well suited for the rapid production of milligrams to tons of products~~ [2, 7, 8]. Such techniques often require multi-

component separation, an initial ~~maximum~~ as high as possible concentration is desired to avoid further costly or even analyte degrading steps to remove the solvent.

In the above applications, the solutes present in a given liquid sample displaced by a miscible displacing fluid in the porous matrix can be retained on the solid phase following the reversible adsorption-desorption step [9]

$$A_m \underset{k_d}{\overset{k_a}{\rightleftharpoons}} A_s. \tag{1}$$

Here, A_m and A_s represent the solute molecules in the mobile and stationary phases respectively, where their concentrations are equal to c_m and c_s, while k_a and k_d are the adsorption and desorption kinetic constants. During the displacement, the solutes are progressively separated because of a selective adsorption of the components on the porous matrix ~~. However, the selectivity of the separation process can be impaired by dispersion mixing processes which cause a broadening of the solute bands and thus possible overlap between the peaks~~ while dispersion causes broadening of the solute bands [9, 5]. In this context, a general goal of the applications mentioned above is to minimize this ~~band broadening~~ concentration overloading related band widening ~~by choosing appropriate operating conditions exploiting variable solute interactions with the porous matrix~~.

The spreading of solutes in a porous matrix is dependent on the adsorption isotherm $c_s = f(c_m)$ expressing the dependence of the solute concentration in the stationary phase c_s on its concentration in the mobile phase c_m [6, 10]. For the linear adsorption isotherm, $c_s = Kc_m$, where $K = k_a/k_d$ is the equilibrium constant of the adsorption-desorption processes. The solute retention is then characterized by the retention factor $k = FK$, where

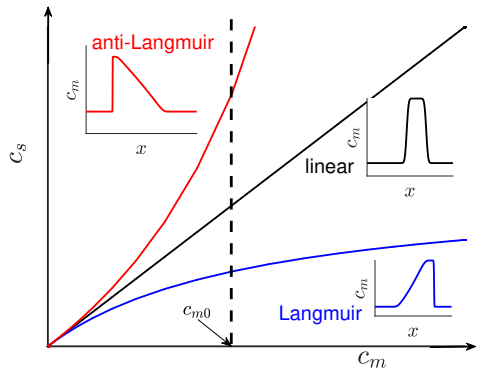

Figure 1: (a) Linear, Langmuir and Anti-Langmuir isotherms with their typical corresponding peak shapes.

$F = V_s/V_m = (1 - \epsilon_{tot})/\epsilon_{tot}$ is the phase ratio of the volume V_s and V_m of the stationary and mobile phases, where ϵ_{tot} is the total porosity or void volume fraction of the porous medium. When the hydrodynamic dispersion and mass transfer limitations are not strong, the linear isotherms result in symmetric solute profiles (see Fig.1). They can typically be used only if the amount of solutes in the sample is sufficiently low [11, 12]. In numerous applications however, the concentration of a component in the stationary phase at equilibrium depends nonlinearly on its concentration in the mobile phase [13]. For a monolayer adsorption, the simplest nonlinear adsorption models are given by Langmuir and anti-Langmuir adsorption isotherms [14].

Langmuir Isotherm

The Langmuir isotherm assumes that, on the porous matrix, there is only a fixed number of sites on which the molecules can adsorb and that these molecules do not interact with the neighbouring sites. The amount of solute needed to saturate the stationary phase in the column thus depends

on the nature of the porous matrix and fixes the saturation capacity of the stationary phase reached when all sites are occupied. The corresponding Langmuir isotherm is expressed as [14]:

$$c_s = \frac{K c_m}{1 + b_L c_m}, \tag{2}$$

where K is the initial slope of the isotherm, b_L is a term related to the adsorption energy; $K/b_L = c_{sat}$ is the monolayer capacity and ~~where $b_L = K/c_{sat}$ represents the rate at which the stationary phase concentration c_s saturates to the saturation capacity c_{sat} and K is the associated adsorption equilibrium constant.~~ Because of this nonlinear adsorption, the velocity of the solute propagation in the mobile phase increases with c_m. This is due to the fact that, when all the adsorption sites are occupied at a sufficiently high concentration, the non-retained solutes at the area of local saturation migrate with a narrow velocity distribution (related to the parabolic flow profile) around the unretained velocity of the mobile phase. Meanwhile the upstream retained solutes experience a much broader distribution of velocities around the average retained velocity as a consequence of the continuous switching between the adsorbed and desorbed states. As a result, a shock layer (SL) forms in the course of time at the frontal interface of the peak [11, 12]. This SL is a thin region of space where the concentration varies continuously but rapidly, and that propagates as a constant pattern [15]. At the rear interface, on the other hand, a rarefaction wave (RF) corresponding to an expanding wave is formed [16] (see Fig.1). On the long term, these two nonlinear waves end up interacting with each other to form an asymptotic triangular peak with a SL at the front, which is a peculiar feature of the Langmuir adsorption isotherm [6, 17].

Anti-Langmuir Isotherm

The anti-Langmuir isotherm is observed in presence of adsorbate-adsorbate interactions favoring further adsorption [18, 19]. Such a cooperativity overloading effect induces an adsorption curve opposite to that of the Langmuir isotherm i.e. c_s increases more rapidly with an increase in c_m (Fig.1). The anti-Langmuir adsorption isotherm is expressed as

$$c_s = \frac{K c_m}{1 - b_{AL}\ c_m}, \tag{3}$$

where b_{AL} is the adsorption parameter. This isotherm is valid provided $c_m \leq c_{th} = 1/b_{AL}$ where c_{th} corresponds to the threshold concentration of the column. Because of the increased adsorption at larger c_m, the velocity of the solute in the mobile phase is smaller in the zones of larger concentrations, which results in the formation of a SL at the rear interface and of a RF wave at the frontal interface [20, 21]. Anti-Langmuir isotherms feature therefore asymptotic triangular peaks with a SL at the back (see Fig.1).

The Langmuir (L) or Anti-Langmuir (AL) models give an appropriate representation of the adsorbed behaviour in many systems [22]. Because of the nonlinear adsorption properties, the tailing at either the rear (L) or frontal (AL) part of the spatial concentration profile enhances the ~~band broadening~~ concentration overloading related band widening and thus impairs the resolution of solute separation or the efficiency of pollution remediation or instance. Efforts are thus being developed to eliminate or reduce the peak tailing effects [23].

~~Deviations to such tailing can be observed in the case of heterogeneous porous matrices [24, 25, 26] containing different zones where the interaction~~

~~of the solid phase with the solute is different. The bi-Langmuir or multi-Langmuir isotherms, the competitive Langmuir isotherm, the Tóth isotherm, and the Freundlich isotherm are a few examples of other models that are then most often used~~ [9, 6]. ~~The simplest model for a heterogeneous adsorption surface is a surface covered with patches exhibiting two different kinds of retention property. The patches are created by covering the surface with different chemical groups which may exhibit a similar interaction isotherm with the solute but with different retention parameter or may exhibit entirely different adsorption isotherms. An example of such surface is found with the chiral stationary phases (CSP) where there is selective retention of one enantiomer with respect to the other one, thus different enantiomers of the same solute show different affinity to the CSP~~ [27]. Alternatively, sharpening of the sample band by applying solvent of modifier gradients ~~using mobile phase gradients of solvent or modifier gradients~~ is a well-known approach to reduce the sample band width [28].

~~On a heterogeneous surface with two different adsorption sites, the peak tailing originating from interaction with both sites is enhanced if one of the adsorption site is weaker than the other one because the molecules are held for a considerable time on the strongly adsorbing site. Thus when desorption occurs, the bulk of the solute zone has already passed over, resulting in the build-up of a tailing part in the concentration profile [29, 30]. A radial heterogeneity can also influence peak tailing in relation to the column efficiency [31].~~

~~An experimental study of heterogeneous surfaces with micropillar array chips reveal a significant increase in band broadening due to disordered arrays~~

~~[32]. The contribution of heterogeneity of support structures flow-through channels has also been demonstrated in an experimental study using ordered and disordered pillar arrays wherein dispersion was measured. Because of the ability to observe dispersion through the transparent glass lid with high precision inside pillar array columns, the effects of overloading have also been clearly observed and these negatively influenced the separation performance [33]. The concentration at which overloading dispersion occurs can be increased as the available specific surface is increased, for which several manufacturing methods are available [34, 35]. This approach however does not fundamentally solve the problem that, at a given concentration, concentration overloading will lead to dispersion and hence dilution or even mixing of the products of interest.~~

In this context, our aim in the present study is to propose and study theoretically a heterogeneous configuration with multi-site adsorption to analyze the conditions on the geometry and adsorption properties of the porous matrix to reduce the solute spreading at overloading concentrations ~~to achieve a better resolution of separated components~~. Specifically, we show that an alternation along the displacement of zones with L or AL adsorption properties can decrease the broadening of peaks thanks to the succession of sharpening of the solute spatial concentration profile at the front or at the rear depending whether the sample crosses a L or an AL zone.

2. Langmuir/Anti-Langmuir (L-AL) adsorption model

We consider a heterogeneous porous matrix consisting of an alternation along the displacement direction x of zones with different adsorption proper-

ties. In some zones, the adsorption on the surface is described by a classical Langmuir isotherm (Eq.2) while the adsorption on the complementary zones of the surface follows an anti-Langmuir isotherm (Eq.3) behavior. The porous matrix is thus composed of alternating bands of two types of sites characterized by different adsorption isotherms. The sites are supposed to behave independently. This is possible for instance when a component like butylbenzene is subject to weak forces of a polar stationary phase. The aromatic analyte-analyte interaction can then dominate, leading to Anti-Langmuir behavior while, in a reverse phase coating, a stronger interaction with the stationary phase will rather give a Langmuir behavior [36, 37, 38]. Our objective is to analyze the influence of this alternation of adsorption properties on the widening of a sample of given initial width L displaced along this sytem at a given velocity U. The flow is assumed to be uniform and the porous matrix is supposed to be radially homogeneous.

2.1. L-AL adsorption isotherm

Local adsorption at a position x and at a time t is given by the isotherm

$$c_s(x,t) = \frac{K c_m(x,t)}{1 + b(x)\ c_m(x,t)}. \tag{4}$$

Depending whether the local site at position x is of the L or AL type, we use

$$b(x) = \begin{cases} b_L, \text{ if } \quad x \in \text{Langmuir zone}, \\ -b_{AL}, \text{ if } \quad x \in \text{anti-Langmuir zone}. \end{cases} \tag{5}$$

The constant b_L quantifies the adsorption-desorption in the Langmuir zone while b_{AL} characterizes the anti-Langmuir sites. As stated before, for the anti-Langmuir isotherm, the function (4) is defined only for $c_m < 1/b_{AL}$. We

define a non-dimensional parameter $\delta = b_L/b_{AL}$ as the ratio of the non-linear adsorption parameters of the Langmuir and anti-Langmuir isotherms.
In this study the following simplifying assumptions are made:

- The adsorption surface is divided equally in Langmuir and Anti-Langmuir zones ~~referred to as plates~~ of equal width L_{plate} covering the column alternatively.
- There is no interaction of the species adsorbed on one type of site with those of the other sites.
- The equilibrium constant K is the same for all ~~plates~~ zones.
- The non-linear adsorption parameter b_L and b_{AL} of the Langmuir and anti-Langmuir ~~plates~~ zones are independent of each other and depend on the threshold mobile phase concentration c_{th} and thus on the porous matrix.
- ~~If $L_{plate} \to 0$, we assume $b(x) \to 0$ and thus we recover the linear adsorption case.~~

Our objective is to achieve reduced peak tailing and hence find the optimal geometrical and adsorption conditions to ~~achieve high efficiency by~~ reduce the ~~band broadening at overloading concentrations~~ concentration overloading related band widening. We next analyze the spreading dynamics of adsorbed solutes on this heterogeneous surface alternating L and AL sites using numerical simulations of the mass balance transfer equation and L-AL isotherms. We show that, with a suitable choice of parameters, the L-AL system leads

to a significant reduction of the solute spreading and can be used to reduce the severe tailing of the concentration profiles.

2.2. L-AL flow model

(Wim and Chinar: I don't understand at all this paragraph. I guess it has been added to please a referee but it makes no sense to me... Can't we suppress it?) Equilibrium theory is an elegant approach to investigate dynamic behavior in chromatography. As it is often justified to assume thermodynamic equilibrium between the mobile and the stationary phase, the governing equations that describe analyte transport can often be appropriately expressed as a system of hyperbolic first-order partial differential equations [11, 12, 22, 39]. As the flow is uniform and the column is assumed to be radially homogeneous, the model is unidimensional. The mass balance equation for the concentration c_m of the solute in the mobile phase and c_s in the stationary phase in presence of advection at speed U and dispersion reads:

$$\frac{\partial c_m}{\partial t} + F\frac{\partial c_s}{\partial t} + U\frac{\partial c_m}{\partial x} = D\frac{\partial^2 c_m}{\partial x^2}, \tag{6}$$

where D is the dispersion coefficient. Taking into account the adsorption isotherm (Eq.4) for c_s and using $k = FK$, the mass balance equation (6) reduces to

$$\frac{\partial}{\partial t}\Big(1 + \frac{k}{(1 + b(x)c_m(x,t))}\Big)c_m(x,t) + U\frac{\partial c_m(x,t)}{\partial x} = D\frac{\partial^2 c_m(x,t)}{\partial x^2}. \tag{7}$$

Let L_x be the length of the uni-dimensional system such that $x \in [0, L_x]$ and x_{in} be the initial position of the rear interface of the sample of width W.

The initial mobile phase concentration $c_m(x,0)$ is then assumed to be

$$c_m(x,0) = \begin{cases} c_{th}/\alpha, \text{ for } \quad x \in [x_{in}, x_{in}+W], \\ 0, \text{ elsewhere,} \end{cases} \tag{8}$$

where $\alpha > 1$. The initial concentration is always assumed to be smaller than c_{th} to avoid the divergence due to anti-Langmuir adsorption. The boundary conditions, imposed on concentration $c_m(x,t)$ and velocity u are:

$$u = U, \quad \frac{\partial c_m(x,t)}{\partial x} = 0, \quad \text{at the inlet and the outlet.} \tag{9}$$

Thus at the boundaries the velocity u is set to be equal to the injection velocity U and a no flux boundary condition is imposed on the mobile phase concentration of the solute.

2.3. Non-dimensionalized L-AL flow model

To nondimensionalize the governing equations, the concentration c_{th} is chosen to non-dimensionalise c_m, b_L and b_{AL}, while U is taken as the characteristic velocity. Defining the length scale $L_c = D/U$ and the time scale $t_c = D/U^2$, the non dimensional velocity, length and time are defined as [40]:

$\hat{U} = U/U = 1, \hat{x} = x/(D/U), \hat{t} = t/(D/U^2)$ while the non-dimensional concentration and adsorption parameters become

$\hat{c}_m = c_m/c_{th}$

$\hat{b}_L = b_L c_{th} = b_L/b_{AL} = \delta,$

$\hat{b}_{AL} = b_{AL} c_{th} = 1$

$$\hat{c}_s = c_s/c_{th} = \begin{cases} \dfrac{K\hat{c}_m}{1+\delta\hat{c}_m}, \text{ if } \quad x \in \text{Langmuir zone,} \\ \dfrac{K\hat{c}_m}{1-\hat{c}_m}, \text{ if } \quad x \in \text{anti-Langmuir zone,} \end{cases}$$

After implementing the above non-dimensionalisation, the mass balance equation becomes:

$$\frac{\partial}{\partial \hat{t}}\Big(1+\frac{k}{(1+\hat{b}(x)\hat{c}_m(x,t))}\Big)\hat{c}_m(x,t)+\frac{\partial \hat{c}_m(x,t)}{\partial \hat{x}}=\frac{\partial^2 \hat{c}_m(x,t)}{\partial \hat{x}^2} \tag{10}$$

where,

$$\hat{b}(x)=\begin{cases}\delta, \text{ for} \quad x\in \text{Langmuir zone},\\ -1, \text{ for} \quad x\in \text{anti-Langmuir zone}.\end{cases} \tag{11}$$

After dropping the hats this can be further simplified and written as :

$$\Big(1+\frac{k}{(1+b(x)c_m(x,t))^2}\Big)\frac{\partial c_m(x,t)}{\partial t}+\frac{\partial c_m(x,t)}{\partial x}=\frac{\partial^2 c_m(x,t)}{\partial x^2} \tag{12}$$

Defining $\kappa=\Big(1+\dfrac{k}{(1+b(x)c_m(x,t))^2}\Big)$, we get finally:

$$\frac{\partial c_m(x,t)}{\partial t}=\frac{1}{\kappa}\frac{\partial^2 c_m(x,t)}{\partial x^2}-\frac{1}{\kappa}\frac{\partial c_m(x,t)}{\partial x}. \tag{13}$$

The non-dimensional length of the domain is $L=UL_x/D$ and the dimensionless length of the L and AL ~~plate~~ zones is $L_p=UL_{plate}/D$. The non-dimensional initial concentration is

$$c_m(x,0)=\begin{cases}1/\alpha, \text{ for} \quad x\in[x_{in},x_{in}+l],\\ 0, \text{ elsewhere},\end{cases} \tag{14}$$

where $l=UW/D_x$ is the non-dimensional width of the injected sample and x_{in} is the initial position of the rear interface of the sample.

2.4. Parameter values and numerical method

The solute mass balance equation (13) is a partial differential equation with variable coefficients that we solve using a Pseudo-spectral Fourier method.

~~The Fourier series expansions of $c_m(x,t)$ and of the right-hand side of equation (13) read:~~ **Chinar, please suppress also eqs.15,16 and 17: I cannot erase them in green**

$$c_m(x,t) = \sum_p \hat{c}_p(t) e^{i(k_p x)} \tag{15}$$

$$J(x,t) = \frac{1}{\kappa}\left\{\frac{\partial^2 c_m}{\partial x^2} - \frac{\partial c_m}{\partial x}\right\} = \sum_p \hat{J}_p(t) e^{i(k_p x)} \tag{16}$$

~~where $k_p = 2\pi p/L\,, (p = 0, 1, 2...)$ are the wave number of Fourier modes. The Fourier coefficients $\hat{c}_p$ are calculated by Fast Fourier Transform with $c_m(x,t)$ known at the collocation points $x_p = (p/M)L,\ p = 0, 1, 2..., M-1$, where M is the number of spectral modes and L is the computational length. Without loss of generality, periodic boundary conditions are taken for $c_m(x,t)$. In Fourier space, equation (13) reduces to a first order ordinary differential equation in time,~~

$$\frac{d\hat{c}_p}{dt} = \hat{J}_p. \tag{17}$$

~~The solution of the above equation (17) is obtained by a predictor-corrector method. The second order Adams-Bashforth method [41] is used to predict the concentration of the solute and the predicted value is corrected by trapezoidal rule. A higher accuracy can be achieved in spectral methods with a coarser mesh that also lead to little or no artificial dissipation.~~ Numerical stability is achieved using $dx = 1, dt = 0.02$, for which the solute mass conservation is also verified. The solutions are observed to remain invariant with further decrease in grid size. The non-dimensional parameters of the problem are α, l, δ, k and L_p that set the initial concentration $c_m(x,0)$, the rate of adsorption and describe the flow dynamics i.e. the propagation pattern of the

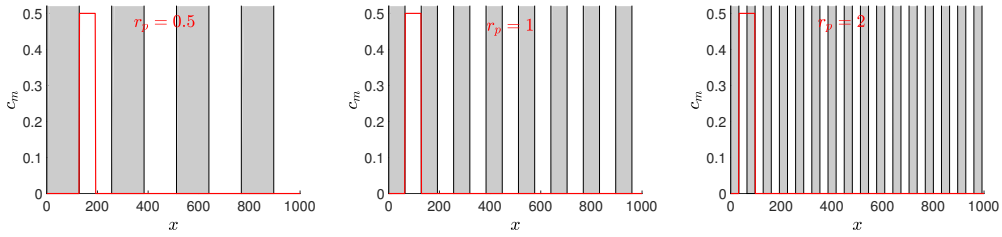

Figure 2: Influence of the parameter $r_p = l/L_p$ on the geometry of the L-AL alternance encountered by the mobile phase concentration profile c_m. The white zones correspond to L ~~plates~~ zones while the grey zones feature AL properties. For a fixed value of l, taken here equal to 64, an increase in r_p corresponds to a decrease of the ~~plate~~ zone width L_p. If $r_p < 1$, the initial sample can be contained within one either pure L or pure AL zone depending on the value of the initial position of the sample given by r_d. Here $r_d = 0$ and the sample starts in a L zone. If $r_p > 1$, the sample initially covers more than one ~~plate~~ zone.

solute and its rate of spreading. In addition to this, the initial position x_{in} of the slice also plays a crucial role in determining the spreading dynamics of the adsorbed solute (as explained in detail in section 3.3).

Since there are a number of variables involved in our model, we combine some variables for which the influence on the propagation dynamics of the solute is observed to be dependent on each other. The values of parameters chosen in the simulations are:

- $\alpha = 2$, which sets the initial mobile phase concentration $c_m(x, 0) = 0.5$.
- The ratio of the width l of the solute slice to the width L_p of the ~~plates~~ zones is $r_p = l/L_p$ (see Figure 2). If $r_p \leq 1$, we study cases for which the sample width l is smaller than or equal to the ~~plate~~ alternation zone width L_p while if $r_p > 1$ then $l > L_p$.

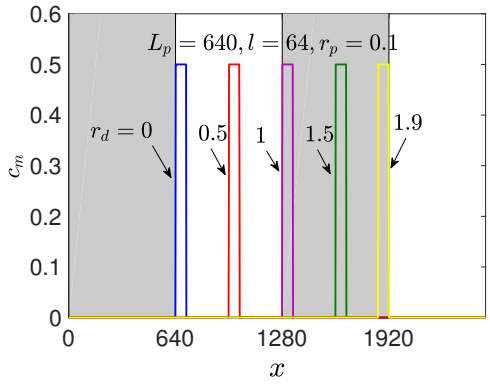

Figure 3: Influence of the parameter r_d on the initial position of the sample for $r_p = 0.1$ here. For $0 < r_d \leq 1$, the rear part of the sample starts in a L zone while for $1 < r_d \leq 2$, the rear part starts in an AL zone.

- The influence of the retention parameter k is studied for $k = 1$ and 5.
- For a given value of x_{in}, the initial condition is observed to repeat itself after $2 * L_p$. The sample is thus assumed to be placed such that its rear starts within the second or third alternation zone i.e. x_{in} is varied as $L_p + r_d * L_p$ with $r_d \in [0, 2)$ (see Figure 3).
- Simulations run up to $t = 50000$ and we fix $l = 64, L = 32768$. So the ratio of the sample length to the column length is $l/L = 0.002$, which is typical of experimental conditions in chromatographic columns.

In the next section, we analyze the influence of varying the parameter values on the propagation and spreading dynamics of the solute.

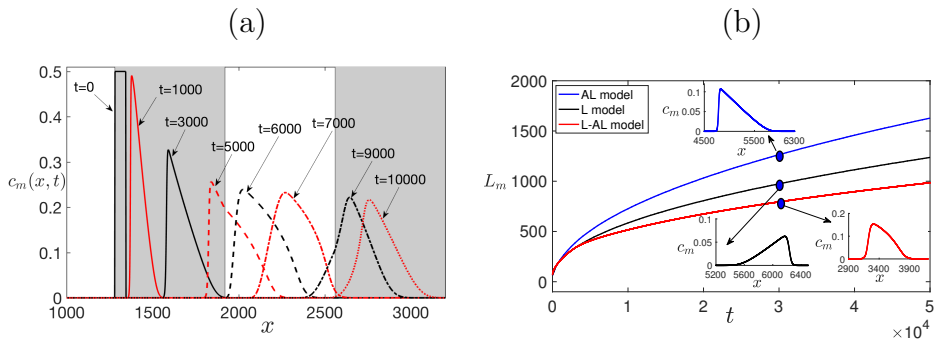

Figure 4: (a) Spatial concentration profiles of the mobile phase $c_m(x,t)$ for $k = 5$ in a L-AL alternate geometry for $b_L = b_{AL} = 1, r_d = 1, r_p = 0.1$ at successive times. (b) Temporal evolution of the spreading length L_m of the adsorbed solute for $k = 5$ in a L model ($b_L = 1$), AL model ($b_{AL} = 1$) and L-AL model ($b_L = b_{AL} = 1, r_p = 0.1, r_d = 1$) with the corresponding peak profiles at the time shown by a bullet.

3. Results

The parameters on which the flow dynamics of the solute depends are here reduced to δ (the ratio b_L/b_{AL} of the nonlinear adsorption parameters), the retention parameter k controlling the strength of the adsorption, the geometrical parameter r_p comparing the relative width of the sample to that of the ~~plates~~ alternation zones and r_d, the parameter controlling whether the initial position of the rear part of the injected sample is in a L or AL zone. Before analyzing the effect of varying the values of these parameters, let us examine the qualitative influence of the alternance of L and AL zones on the dynamics.

3.1. Accordion effect and reduction of peak widening

Fig.(4)a shows a typical displacement of a finite width sample into a L-AL alternating geometry. We take here $k = 5$ corresponding to a quite

strong adsorption effect and $\delta = 1$ for $b_L = b_{AL} = 1$ i.e. the adsorption parameter is of the same strength in the L and AL ~~plates~~ zones. The width l of the sample is 1/10 of the length L_p of the ~~plates~~ L/AL zones such that the geometrical parameter $r_p = l/L_p = 0.1$. For $r_d = 1$, the left part of the sample starts at the initial time in an AL zone and, as $r_p < 1$, the sample is initially totally contained in the AL zone (see Fig. 4(a) at time $t = 0$). Once the displacement starts, the rear part of the sample is sharpening while its frontal is widening because of the anti-Langmuir adsorption properties of the ~~plate~~ AL zone in which the sample starts its journey in the porous matrix (see Fig. 4(a) at times $t = 1000, 3000$). However, once the sample starts passing through a L zone, the reverse effect sharpens its front while diluting the rear part (see Fig. 4(a) at times $t = 5000, 6000, 7000$). The alternation between sharpening and widening at both edges of the sample gives an accordion effect that, in the end, reduces the total broadening of the peak. This can be appreciated in figure 4(b) giving the temporal evolution of the spreading length L_m, computed as the length of the interval for which the solute concentration $c_m \geq 0.001$ [42]. L_m is a measure of the widening of the peak. First, we note that the pure AL displacement gives a larger broadening of the sample than a pure L one because, for AL displacements, the rarefaction wave is formed in the direction of the flow, thus spreading due to rarefaction is further enhanced. The peak profiles for L and AL displacements at time $t = 3 \times 10^4$ are shown in the inset of Fig. 4(b) [21]. It is seen that the L-AL alternation gives a smaller mixing length at a given time than both pure L or AL systems, thanks to this accordion effect. Let us now see how this reduction of peak widening in the L-AL system depends

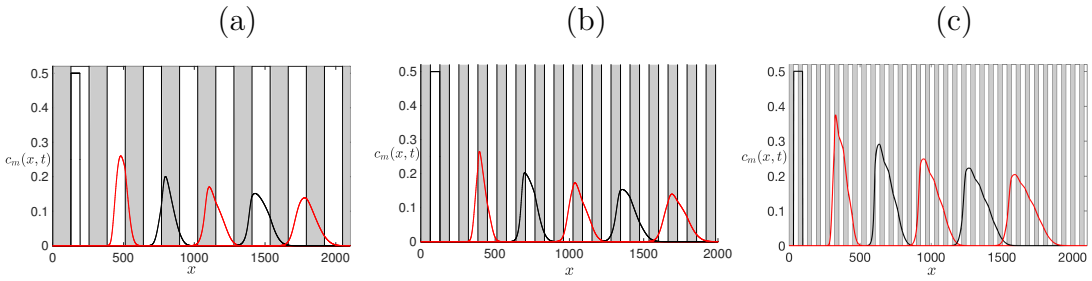

Figure 5: Spatial concentration profiles in the mobile phase $c_m(x,t)$ for $k = 5, \delta = 1$ with $b_L = b_{AL} = 1, r_d = 0$ and (a) $r_p = 0.5$ (b) $r_p = 1$ (c) $r_p = 2$ at times $t = 0, 2000, 4000, 6000, 8000, 10000$.

on the various parameters of the problem.

3.2. Influence of r_p

Figure (5) shows the concentration profiles $c_m(x,t)$ of the solute in the mobile phase for different values of r_p when the other parameter values are fixed. When the ~~plate~~ alternation zone width is larger than the initial sample width i.e. $r_p \leq 1$, the solute peak shape behaves in an Anti-Langmuir way in the AL-~~plates~~ zones and smoothly switches to a Langmuir behavior in the L ~~plates~~ zones (see figure 5(a)-(b)). On the contrary, when $r_p > 1$, the solute concentration distribution encounters rapid local expansions and contractions whenever the ~~plate~~ zone switch happens inducing undulated profiles (see figure 5(c)). The temporal evolution of the spreading length L_d given in figure 6 shows that the solute spreading for the L-AL models is always smaller for all r_p scanned than for transport in the single site adsorption Langmuir or anti-Langmuir systems. This is because the peak tailing, which results in ~~band broadening~~ concentration overloading related band widening of the Langmuir or anti-Langmuir adsorbed solute, is prominently reduced

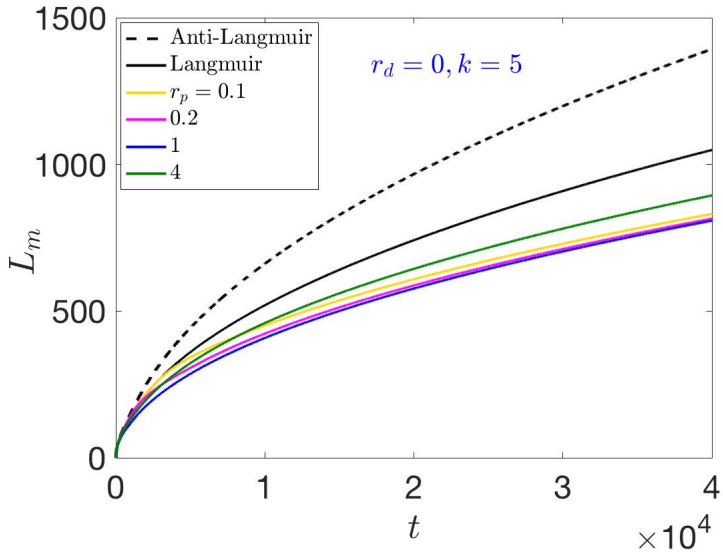

Figure 6: Temporal evolution of the spreading length L_m of the adsorbed solute for different values of r_p, at fixed $r_d = 0, k = 5, \delta = 1$.

with the alternance of L and AL ~~plates~~ zones. In addition, in the L-AL model, L_m varies with r_p. It is observed that L_m is smaller for $0 < r_p \leq 1$ in comparison to $r_p > 1$ cases. Thus least spreading in the L-AL system can be obtained when the width of the sample is smaller than the width of the ~~plate~~ alternation zones i.e. $l < L_p$. In the limiting case of $r_p \to 0$, or equivalently $L_p \to \infty$ for a finite l, the solute profile depicts the features of a single site model of either Langmuir or anti-Langmuir properties depending upon the initial position of the sample. On the other hand, for $r_p \to \infty$ or also $L_p \to 0$, we recover symmetric solute peaks as in the case of linear adsorption.

3.3. Influence of r_d

In the L-AL system, we find that the initial position of the sample i.e. whether it is initially injected into a L or an AL ~~plate~~ zone has an influence

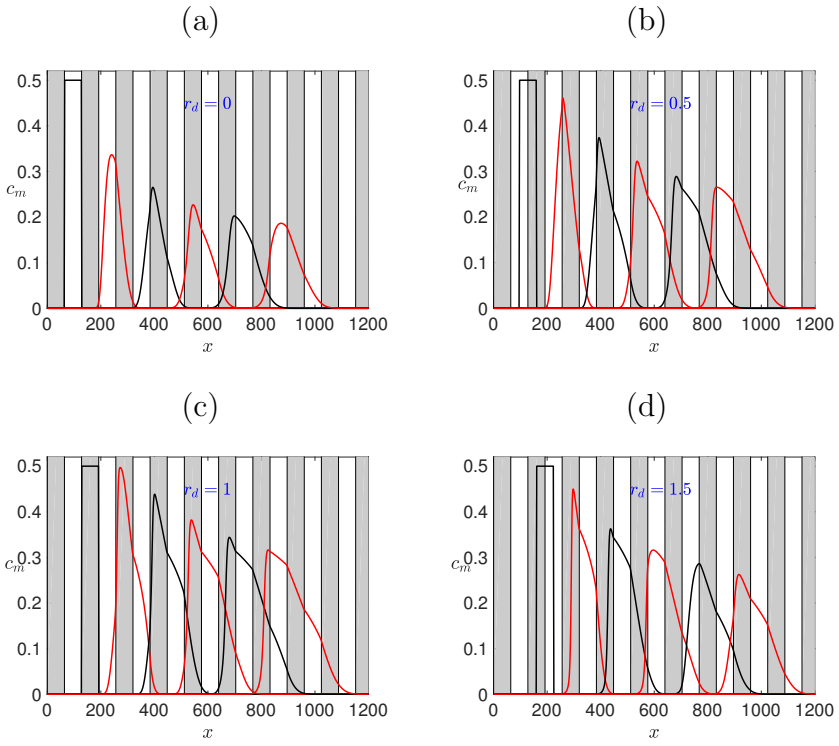

Figure 7: Concentration profiles in the mobile phase c_m with $r_p = 1, \delta = 1, k = 5$ for (a) $r_d = 0$ (b) $r_d = 0.5$ (c) $r_d = 1$ (d) $r_d = 1.5$ at times $t = 0, 1000, 2000, 3000, 4000, 5000$.

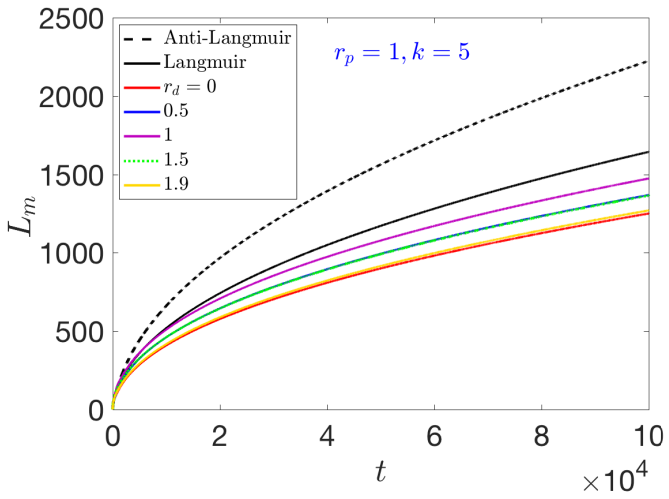

Figure 8: Temporal evolution of the spreading length L_m for different initial position r_d of the sample for $r_p = 1$, $\delta = 1$ and $k = 5$

on the peak profile and on the spreading dynamics of the adsorbed solute. This can be appreciated in figure (7) giving the spatial concentration profiles of the solute in the mobile phase at successive times for different values of r_d for $k = 5, b_L = b_{AL} = 1, r_p = 1$. Depending on the initial position of the sample i.e. depending on r_d, a difference is observed in the amplitude and shape of the solute peak. During the propagation, the width of the flat top solute decreases and, following the interaction of the two interfaces, becomes a point. After that, the solute peak height starts decreasing from the initial concentration $1/\alpha$ in the course of time. Therefore, if the initial position of the solute sample in a L-AL system is such that both interfaces undergo widening in the early times (for instance if the frontal part of the sample is in an AL zone while its rear is in a L zone), the peak height starts decreasing faster. On the contrary, if the initial position of the solute sample is such that

both interfaces undergo sharpening in the early times (for instance frontal part in L and rear part in AL), then the decrease of the peak height occurs later. For instance, in Figure 7(a), with $r_d = 0$, the frontal and rear interfaces of the solute both undergo expansion when the displacement starts as they spend the early times in the AL ~~plate~~ zone and L ~~plate~~ zone, respectively. This results in their early interaction and a faster decrease of the amplitude of the solute peak with time. In Figure 7(c), we see that with $r_d = 1$, the frontal and rear of the solute undergo initially sharpening as they spend early times in the L ~~plate~~ zone and AL ~~plate~~ zone, respectively. This results in their late interaction and a delayed decrease in the amplitude of the solute peak with time. The smallest amplitude is therefore observed for $r_d = 0$ and the largest one for $r_d = 1$. Intermediate situations are obtained for other values of r_d (see Figure 7b, 7d). Since the initial position of the solute determines the early time interaction of the solute with the L-AL alternation, it has thus an effect on the amplitude of the solute.

The corresponding temporal evolution of the spreading length L_m given in Figure 8 shows again that L_m is always smaller for the L-AL model than in the single site Langmuir or anti-Langmuir systems. In addition, in the L-AL model, L_m varies with r_d: L_m grows non-monotonically with r_d i.e., for $0 \leq r_d \leq 1$, L_m increases with r_d, while it decreases for $1 < r_d < 2$. For $r_p = 1$ the smallest width is obtained for $r_d = 0$. Thus the most efficient situation in terms of decreasing ~~band broadening~~ concentration overloading related band widening is thus to start in a L ~~plate~~ zone. This suggests that the solute dynamics carries its history along the displacement for a long time when passing through alternating L and AL ~~plates~~ zones.

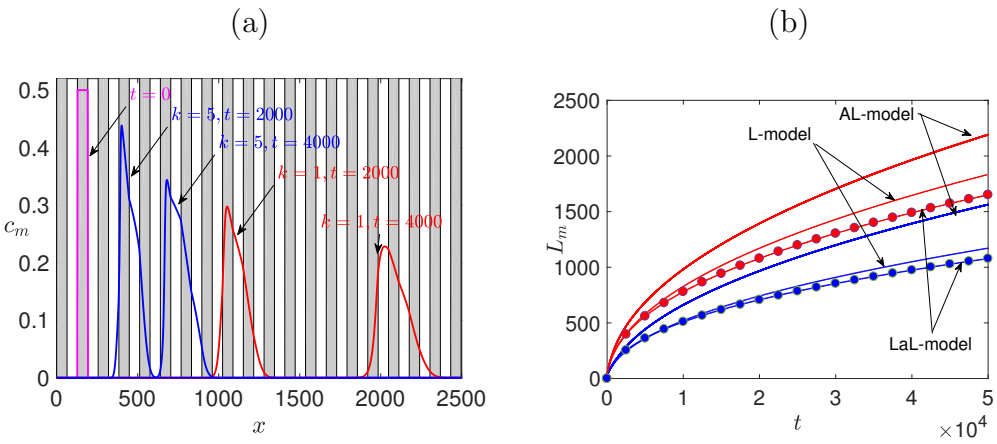

Figure 9: (a) Concentration profiles in the mobile phase c_m at different times for $k = 1$ (red) and $k = 5$ (blue) with $r_d = 1, r_p = 1, \delta = 1$. (b) Temporal evolution of the corresponding spreading length L_m and comparison with the pure L and AL cases.

(Chinar, In Fig.9b, "LaL-model" in the figure should be replaced by "L-AL model". Also suppress the hyphen in "L-model" to read "L model". Idem with "AL-model": it should be "AL model")

3.4. Influence of k on the solute spreading

For a linear adsorption, it has been shown that the larger the value of the retention parameter k, the more the solute is retained on the porous matrix and thus the slower it propagates [43]. In the case of L-AL alternance, larger values of k imply that the sample will interact with each ~~plate~~ zone more strongly and will thus be more influenced by the multiple adsorption site situation in comparison to the small values of k.

This can be appreciated on figure 9(a) comparing the concentration profiles $c_m(x,t)$ at different times for $k = 1$ and 5 keeping r_p, δ and r_d fixed. We

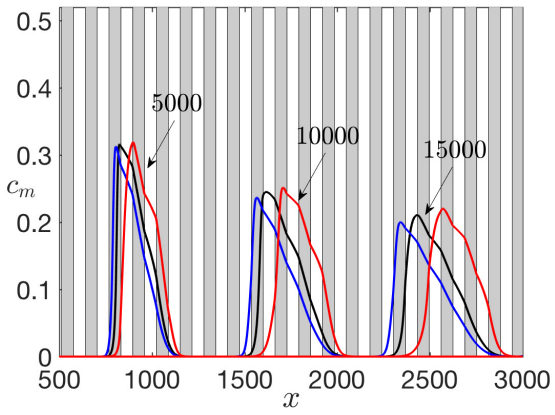

Figure 10: Concentration profiles in the mobile phase c_m for $k = 5$ at different times for $\delta = 0.5$ (blue), 1 (black) and 2 (red) with $r_d = 1, r_p = 1$.

see that, for $k = 5$, the stronger retention on the porous matrix induces a slower transport of the sample, a stronger influence of the L-AL alternation and a smaller broadening than with $k = 1$. The longer interaction time of the solute with the corresponding ~~plates~~ zones when k is larger favors thus a more efficient accordion effect leading to better resolved peaks. This is confirmed by analyzing the spreading length of the adsorbed solute for different L_m for these two values of k as plotted in figure 9(b). L_m is always smaller for the L-AL model than for the pure L or AL cases, irrespective of the value of k and the smallest widening for the L-AL system is obtained for larger k.

3.5. Influence of δ on the solute spreading

The non-dimensional parameter $\delta = b_L/b_{AL}$ compares the strength of the non-linear adsorption on Langmuir ~~plates~~ zones to the one on anti-Langmuir ~~plates~~ zones. If $\delta = 1$, we have $b_L = b_{AL}$, which implies that the magnitude of the deviation from a linear adsorption behavior is identical for both studied

cases (with however opposite signs, resulting in Langmuir and Anti-Langmuir behavior, respectively). If δ is increased above one, the influence of L ~~plates~~ zones is more and more pronounced with regard to that of the AL ~~plates~~ zones and, vice-versa, for $\delta < 1$, AL ~~plates~~ zones dominate the solute transport dynamics. To illustrate this, Figure 10 compares the concentration profiles of the solute for $\delta = 0.5, 1, 2$. We see that, for $\delta = 0.5$, the rear of the sample tends to a shock wave while the frontal part has more tailing, which shows the dominance of the AL ~~plates~~ zones. On the contrary, for $\delta = 2$, the L ~~plates~~ zones can counteract this and "redress" the profile to reach a more symmetric peak shape.

Thus, for the applications where reducing the ~~band broadening~~ concentration overloading related band widening of the solute is essential to increase the efficiency of the method, an alternation of L and AL ~~plates~~ zones provides a robust mechanism to reduce the spreading of the solute. It remains to assess more quantitatively which combinations of the four parameters gives the best reduction of peak broadening. This is analyzed in the next section where ~~an optimization~~ a strategy to reduce the peak broadening is proposed.

4. Quantitative analysis

From the above results, it is clear that the global features of the solute displacement in a L-AL system, like the widening of the solute peaks, are largely controlled by the adsorption parameters (k, δ) but also by the parameters r_p and r_d related to the geometry of the alternation between the L and AL ~~plates~~ zones.

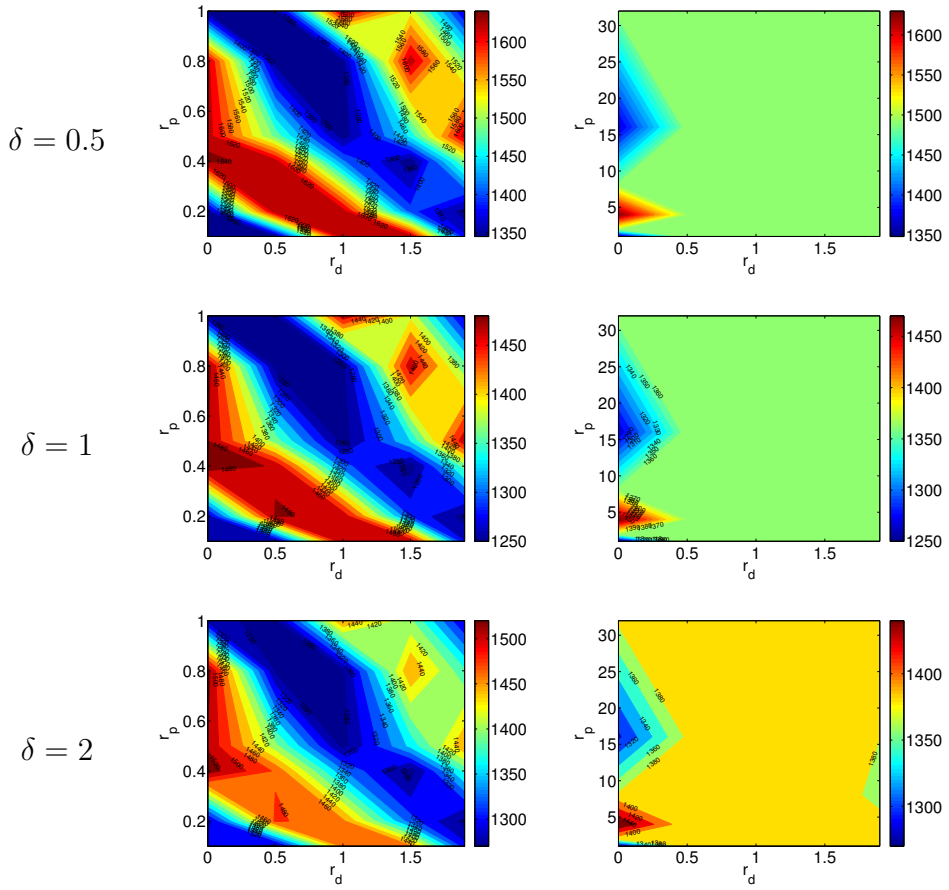

Figure 11: Phase diagrams giving the values of L_m at $t = 10^5$ in the (r_p,r_d) phase space for $k = 5$ and different values of δ. The left column refers to the case $r_p \leq 1$ while, in the right one, we have $r_p > 1$.

~~In order to have a better overview of the effect of varying r_p and r_d on the efficiency of decreasing the peak widening, we next plot in~~ Figures 11 and 12 show phase diagrams giving the amplitude of the spreading length L_m at the final time of the simulation in the parameter space (r_p,r_d) for $k = 1$ or 5 and 3 different values of δ. The colors on the graph vary from red for the (r_p, r_d)

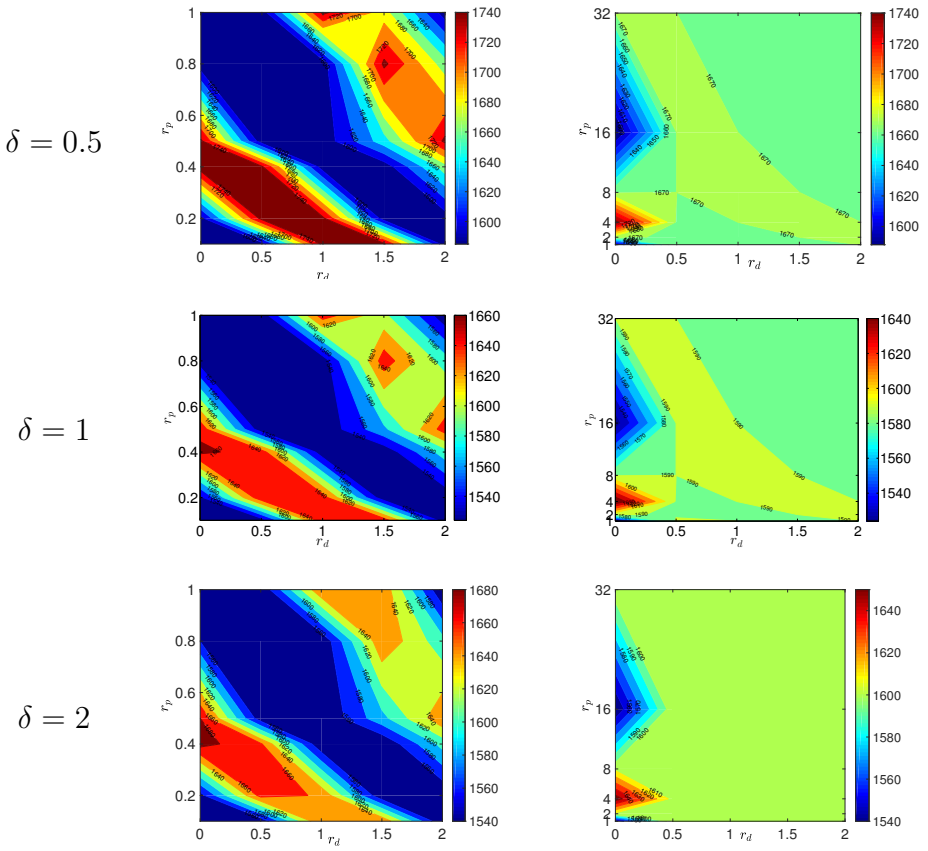

Figure 12: Phase diagrams giving the values of L_m at $t = 50000$ in the (r_p,r_d) phase space for $k = 1$ and different values of δ. The left column refers to the case $r_p \leq 1$ while, in the right one, we have $r_p > 1$.

couple of parameters at which L_m is maximum to blue for the minimal L_m values. The absolute values of L_m for a given color is given in the color bar to the right of each panel but in all cases red and blue correspond to the maximum and minimum values.

4.1. Quantitative analysis of spreading lengths values

Figures 11 and 12 show the phase diagrams of L_m for $k = 5$ and $k = 1$ respectively for three different values of δ. To be able to compare the situation with a single site model, we fixe $b_{AL} = 1$ and vary b_L to get different values of $\delta = b_L/b_{AL}$. Specifically, we take $b_L = 0.5, 1$ and 2 to get the values $\delta = 0.5, 1, 2$ respectively.

The phase diagrams show a large variation of the final values of L_m when $r_p \leq 1$ (left column) for all values of r_d and δ. On the contrary, for $r_p > 1$ (right column), the spreading length remains in a particular color zone for $r_d > 0.5$. This shows that the influence of r_d is more pronounced on the solute spreading when the ~~plate~~ alternation zone width L_p is larger than the sample width l. Nevertheless, in all heterogeneous cases, the widening of the peak is smaller than the one in a pure homogeneous L or AL system. To appreciate this, we compare in Table 1 the spreading length L_L or L_{AL} at the final time t_{fin} for a single L or AL site model respectively, with the least spreading L_{min} and maximum spreading L_{max} obtained at the same time in the L-AL model. We see that in the L-AL cases, the width of the solute peaks is always smaller than that of the pure L or AL cases. The gain in peak width reduction varies however with the specific combination of the parameter values. To quantify the gain in peak width reduction we compute the percentage of maximum gain compared to a pure AL column as $G_{AL} = \dfrac{L_{AL} - L_{min}}{L_{AL}} \times 100$. A gain of decrease in peak width as high as 43.82% for L-AL displacement in comparison to a single AL site model is achieved. A similar measure gives the gain with respect to a pure L column as $G_L = \dfrac{L_L - L_{min}}{L_L} \times 100$. A maximum gain of 32.20% in decrease in peak

k	δ	t_{fin}	L_L	L_{AL}	L_{min}	L_{max}	G_{AL}	G_L
5	0.5	10^5	1463	2225	1347	1646	39.46	7.93
5	1	10^5	1645	2225	1250	1500	43.82	24.01
5	2	10^5	1876	2225	1272	1530	42.83	32.20
1	0.5	5×10^4	1663	2192	1586	1754	27.65	4.63
1	1	5×10^4	1830	2192	1524	1665	30.47	16.72
1	2	5×10^4	2096	2192	1540	1688	29.74	26.53

Table 1: Table of L_m at t_{fin} for different values of k, δ at fixed $b_{AL} = 1$ and variable b_L in the case of a pure Langmuir (L_L) or Anti-Langmuir (L_{AL}) systems. L_{min} and L_{max} give the minimum and maximum values of L_m for an L-AL system when (r_p, r_d) are varied (see Figure 11 and 12).

width for L-AL displacement is achieved in comparison to a single L site model.

4.2. Strategy to reduce the peak broadening

The above results allow to design optimal L-AL heterogeneity configurations of chromatographic column or optimal configurations for practical engineering applications to reduce the mixing length of the solute. Although the L-AL model always results in a smaller solute spreading than the classical single site model, an improved performance can be obtained by a suitable choice of optimal ~~plate~~ alternation zone width to sample width ratio, optimal choice of initial zone in which to start the injection and relative strengths of the L/AL ~~plates~~ zones. As stated previously, different combinations of r_p and r_d affect dramatically the performance of the L-AL model. We have

explored a large number of different configurations looking for a maximum output efficiency. We find that the combinations of r_d and r_p giving the maximal reduction in ~~band broadening~~ concentration overloading related band widening are the following :

- For $r_d \in [0, 0.5]$, $r_p \in (0, 0.2] \cup [0.8, 1] \cup (8, 32)$.
- For $r_d \in [0.5, 1.5], r_p \in [0.4, 0.8]$.
- For $r_d \in [1.5, 2], r_p \in (0, 0.4]$.

The larger the values of k, the larger the effect of this reduction in sample spreading.

5. Conclusion

We have analyzed theoretically the transport properties of a sample of solute injected in a heterogeneous porous matrix alternating in space regions featuring Langmuir (L) and Anti-Langmuir (AL) adsorption isotherms. ~~Depending whether the solute experiences locally a L or AL adsorption environment, broadening of its concentration in the mobile phase occurs at different speed. Indeed, in a L environment, the frontal part of the spatial solute concentration profile sharpens while its rear is broadening. A reverse formation of a shock at the rear with rarefaction at the frontal part of the spatial peak characterizes the AL dynamics. We have shown that, in a heterogeneous L-AL system, the solute encounters an alternation in space of these two different behaviors inducing~~ This alternation induces an accordion effect reducing the ~~band broadening~~ concentration overloading related

band widening of the peak. We have developed a theoretical model describing displacement in this L-AL system in which the important parameters of the problem are the adsorption parameter $\delta = b_L/b_{AL}$ comparing the intensity of the nonlinear adsorption isotherm parameters, the retention parameter k controlling the strength of the adsorption, the geometrical parameter $r_p = l/L_p$ comparing the relative width l of the sample to the length L_p of the ~~plates~~ L/AL zones and r_d, the parameter controlling whether the position of the rear part of the injected sample is in a L or AL zone at $t = 0$.

We find that, whatever the values of the parameters scanned here, the L-AL alternation always give a smaller peak broadening than the pure L or AL cases. The widening reduction increases when the adsorption intensity k increases. The geometry of the L-AL alternation is found to have an important influence. If the width of the ~~plates~~ L/AL zones is very small (i.e. r_p tends to infinity), the accordion effect cannot be effective and the system recovers symmetric profiles typical of linear adsorption. On the contrary, pure L or AL systems are recovered for very large ~~plates~~ zones ($r_p \to 0$) depending whether the sample is injected into a L or AL zone. For intermediate values of r_p, broadening reduction is obtained, the efficiency of which further depends on the zone in which the sample is injected initially, which is controlled by the parameter r_d. If the sample width and value of r_d are such that the frontal part of the sample experiences at the beginning of the displacement a sharpening in a L zone while its rear also sharpens because it crosses at early times an AL zone, then the widening effect is delayed and the peak broadening will be the smallest. A further control of the relative weight of the L or AL behavior can be obtained by tuning the parameter δ. We have

performed a characterization of the influence of varying these various parameters on the dynamics and have given their optimal combination of values to reduce the concentration overloading related band widening. Our results pave the way to developing new heterogeneous porous matrices alternating zones of different adsorption properties to optimize the reduction of ~~band broadening~~ concentration overloading related band widening. The concept is quite general. We have demonstrated it here with an alternation of two zones with Langmuir and Anti-Langmuir adsorption properties of equal width but the analysis can be straightforwardly adapted to more complex geometries with ~~plates~~ zones of different lengths and with different adsorption isotherms. Allowing for more than two different adsorption regimes will further increase the possible selectivity of the control strategy. Experimental demonstration of the efficiency of our theoretical concepts could for instance be obtained using micro-pillar array chips [34, 35] ~~and should be easy to implement in a large number of applications~~.

References

[1] B. Metz, O. Davidson, H. de Coninck, M. Loos, L. A. Meyer (Eds.), IPCC Special Report on Carbon Dioxide Capture and Storage, Cambridge University Press, 2005.

[2] R. Farajzadeh, A. Andrianov, R. Krastev, G. J. Hirasaki, W. R. Rossen, Foam–oil interaction in porous media: Implications for foam assisted enhanced oil recovery, Advances in Colloid and Interface Science 183-184 (2012) 1–13.

[3] L. Lüehrmann, U. Noseck, C. Tix, Model of contaminant transport in porous media in the presence of colloids applied to actinide migration in column experiments, Water Resources Research 34 (3) (1998) 421–426.

[4] L. M. Abriola, Modeling contaminant transport in the subsurface: An interdisciplinary challenge, Reviews of Geophysics 25 (2) (1987) 125.

[5] R.-M. Nicoud, Chromatographic Processes: Modeling, Simulation, and Design, Cambridge University Press, 2015.

[6] G. Guiochon, A. Felinger, D. G. Shirazi, A. M. Katti, Fundamentals of Preparative and Nonlinear Chromatography, Elsevier Science, 2006.

[7] J. D. Seader, E. J. Henley, D. K. Roper, Separation Process Principles: Chemical and Biochemical operations, John Wiley and Sons Ltd, 2010.

[8] D. Broseta, F. Medjahed, J. Lecourtier, M. Robin, Polymer adsorption/retention in porous media: Effects of core wettability and residual oil, SPE Advanced Technology Series 3 (01) (1995) 103–112.

[9] D. M. Ruthven, Principles of Adsorption and Adsorption Processes, Wiley-Interscience, 1984.

[10] D. De Vault, The theory of chromatography, Journal of American chemical Society 65 (1943) 532–540.

[11] H.-K. Rhee, R. Aris, N. R. Amundson, First-Order Partial Differential Equations: Volume I: Theory and Applications of Single Equations, Prentice-Hall, Inc., 1986.

[12] H.-K. Rhee, R. Aris, N. R. Amundson, First-order Partial Differential Equations. Vol. 2: Theory and Application of Hyperbolic Systems of Quasilinear Equations, Prentice-Hall, Inc., Upper Saddle River, NJ, USA, 1989.

[13] F. Gritti, G. Guiochon, Critical contribution of nonlinear chromatography to the understanding of retention mechanism in reversed-phase liquid chromatography, Journal of Chromatography A 1099 (1-2) (2005) 1–42.

[14] C. H. Giles, D. Smith, A. Huitson, A general treatment and classification of the solute adsorption isotherm. i. theoretical, Journal of Colloid and Interface Science 47 (3) (1974) 755–765.

[15] G. B. Whitham, A new approach to problems of shock dynamics part i two-dimensional problems, Journal of Fluid Mechanics 2 (02) (1957) 145.

[16] F. G. Helfferich, P. W. Carr, Non-linear waves in chromatography: I. waves, shocks, and shapes, Journal of Chromatography 629 (1993) 97–122.

[17] C. Rana, S. Pramanik, M. Martin, A. De Wit, M. Mishra, Viscous fingering and nonlinear wave interactions, arXiv:1808.00699.

[18] A. Cavazzini, G. Bardin, K. Kaczmarski, P. Szabelski, M. Al-Bokari, G. Guiochon, Adsorption equilibria of butyl- and amylbenzene on monolithic silica-based columns, Journal of Chromatography A 957 (2) (2002) 111–126.

[19] S. Golshan-Shirazi, G. Guiochon, Experimental study of the elution profiles of high concentration bands of binary mixtures eluted by a binary eluent containing a strongly retained additive, Analytical Chemistry 61 (21) (1989) 2380–2388.

[20] B. Lin, T. Yun, G. Zhong, G. Guiochon, Shock layer analysis for a single-component in preparative elution chromatography, J. Chromatography A 708 (1995) 1–12.

[21] C. Rana, M. Mishra, A. De Wit, Effect of anti-langmuir adsorption on spreading in porous media, EuroPhysics Letters (submitted).

[22] M. Mazzotti, Equilibrium theory based design of simulated moving bed processes for a generalized langmuir isotherm, Journal of Chromatography A 1126 (1) (2006) 311 – 322.

[23] V. R. Meyer, Practical High-performance Liquid Chromatography, John Wiley & Sons, 2010.

[24] J. Jacobson, J. Frenz, C. Horváth, Measurement of adsorption isotherms by liquid chromatography, J. Chromatogr. A 316 (1984) 53 – 68.

[25] L. K. Koopal, W. H. van Riemsdijk, J. C. M. de Wit, M. F. Benedetti, Analytical isotherm equations for multicomponent adsorption to heterogeneous surfaces, Journal of Colloid and Interface Science 166 (1) (1994) 51–60.

[26] S.-B. Kim, M. Y. Corapcioglu, Contaminant transport in dual-porosity media with dissolved organic matter and bacteria present as mobile colloids, Journal of Contaminant Hydrology 59 (3-4) (2002) 267–289.

[27] T. J. Ward, K. D. Ward, Chiral separations: A review of current topics and trends, Analytical Chemistry 84 (2) (2012) 626–635.

[28] J. C. Strong, D. D. Frey, Experimental and numerical studies of the chromatofocusing of dilute proteins using retained pH gradients formed on a strong-base anion-exchange column, Journal of Chromatography A 769 (2) (1997) 129 – 143.

[29] J. C. Giddings, Kinetic origin of tailing in chromatography., Analytical Chemistry 35 (13) (1963) 1999–2002.

[30] T. Fornstedt, G. Zhong, G. Guiochon, Peak tailing and slow mass transfer kinetics in nonlinear chromatography, Journal of Chromatography A 742 (1-2) (1996) 55–68.

[31] K. Miyabe, G. Guiochon, Peak tailing and column radial heterogeneity in linear chromatography, Journal of Chromatography A 830 (2) (1999) 263–274.

[32] H. Eghbali, V. Verdoold, L. Vankeerberghen, H. Gardeniers, G. Desmet, Experimental investigation of the band broadening arising from short-range interchannel heterogeneities in chromatographic beds under the condition of identical external porosity, Analytical Chemistry 81 (2) (2009) 705–715.

[33] J. Op De Beeck, M. Callewaert, H. Ottevaere, H. Gardeniers, G. Desmet, W. De Malsche, On the advantages of radially elongated structures in microchip-based liquid chromatography, Analytical Chemistry 85 (10) (2013) 5207–5212.

[34] S. Futagami, T. Hara, H. Ottevaere, G. V. Baron, G. Desmet, W. De Malsche, Preparation and evaluation of mesoporous silica layers on radially elongated pillars, Journal of Chromatography A 1523 (2017) 234–241.

[35] M. Callewaert, J. Op De Beeck, K. Maeno, S. Sukas, H. Thienpont, H. Ottevaere, H. Gardeniers, G. Desmet, W. De Malsche, Integration of uniform porous shell layers in very long pillar array columns using electrochemical anodization for liquid chromatography, The Analyst 139 (3) (2014) 618–625.

[36] F. Gritti, W. Piatkowski, G. Guiochon, Comparison of the adsorption equilibrium of a few low-molecular mass compounds on a monolithic and a packed column in reversed-phase liquid chromatography, Journal of Chromatography A 978 (1) (2002) 81 – 107.

[37] F. Gritti, G. Guiochon, Repeatability and reproducibility of high concentration data in reversed-phase liquid chromatography: I. overloaded band profiles on kromasil-c18, Journal of Chromatography A 1003 (1) (2003) 43 – 72.

[38] T. Fornstedt, G. Götmar, M. Andersson, G. Guiochon, Dependence on the mobile-phase ph of the adsorption behavior of propranolol enantiomers on a cellulase protein used as the chiral selector, Journal of the American Chemical Society 121 (6) (1999) 1164–1174.

[39] F. Ortner, L. Joss, M. Mazzotti, Equilibrium theory analysis of liquid

chromatography with non-constant velocity, Journal of Chromatography A 1373 (2014) 131 – 140.

[40] G. M. Homsy, Viscous fingering in porous media, Annual Review of Fluid Mechanics 19 (1987) 271–311.

[41] J. C. Butcher, Numerical Methods for Ordinary Differential Equations, John Wiley & Sons, 2003.

[42] A. De Wit, Y. Bertho, M. Martin, Viscous fingering of miscible slices, Physics of Fluids 17 (5) (2005) 054114.

[43] M. Mishra, M. Martin, A. De Wit, Influence of miscible viscous fingering of finite slices on an adsorbed solute dynamics, Physics of Fluids 21 (8) (2009) 083101.